Available online at www.sciencedirect.com

ScienceDirect

Journal of Nutritional Biochemistry 107 (2022) 109052

Journal of Nutritional Biochemistry

RESEARCH PAPER

Excess fructose enhances oleatic cytotoxicity via reactive oxygen species production and causes necroptosis in hepatocytes

Jo Kanazawa[a], Keisuke Kakisaka[a,*], Yuji Suzuki[a], Takehiro Yonezawa[a], Hiroaki Abe[a], Ting Wang[b], Yasuhiro Takikawa[a]

[a] Division of Hepatology, Department of Internal Medicine, School of Medicine, Iwate Medical University, Yahaba-cho, Iwate, Japan
[b] Division of Biomedical Research and Development, Institute of Biomedical Sciences, Iwate Medical University, Yahaba-cho, Iwate, Japan

Received 14 February 2021; received in revised form 30 March 2022; accepted 6 April 2022

Abstract

Non-alcoholic fatty liver disease (NAFLD), the hepatic phenotype of metabolic syndrome, has been identified as a major health concern as the number of cirrhosis and deaths associated with NAFLD is expected to increase. Although fructose intake has been considered to be a progressive factor in the pathophysiology of NAFLD, it remains unclear how fructose contributes to hepatocellular damage during lipotoxicity. In the present study, we aimed to analyze the hepatotoxicity of fructose in steatosis. Fructose effects on lipotoxicity were evaluated in HepG2 cells, primary mouse hepatocytes, and in mice fed a high-fat diet with or without sucrose (HFDS/HFD). Oleate induced caspase 3-independent cell death in HepG2 cells and primary mouse hepatocytes cultured in fructose-supplemented medium, and induced cleavage of caspase-1 in primary mouse hepatocytes. In addition, the number of cells stained positive for reactive oxygen species (ROS) was significantly increased, and N-acetyl cysteine was found to inhibit ROS production and cell death. Cell death was confirmed to be through necrotic cell death, and phosphorylation of mixed lineage kinase domain-like (MLKL) protein was observed. Taken together, hepatocyte cytotoxicity was due to excess fructose with oleate-induced ROS-mediated necroptosis. HFDS mice showed progressive hepatic fibrosis and inflammation and a higher NAS score than HFD mice or mice fed a control diet. The expression of hemoxygenase-1, phosphorylation of MLKL, cleavage of caspase1, and apoptosis were significantly increased in the livers of mice fed a HFDS. Overall, excess fructose intake induces necroptosis through the production of ROS and enhances the toxicity of oleatic cytotoxicity.
© 2022 Elsevier Inc. All rights reserved.

Keywords: Non-alcoholic fatty liver disease; High-fat diet; Fructose; Necroptosis; Lipotoxicity.

1. Introduction

The incidence of metabolic syndrome due to obesity and insulin resistance is increasing worldwide [1,2]. Non-alcoholic fatty liver disease (NAFLD), the hepatic phenotype of metabolic syndrome, is also increasing [3,4]. After successful eradication of hepatitis virus C by direct acting antivirals, NAFLD is one of the leading causes of liver cirrhosis [5]. Therefore, the increasing occurrence of NAFLD is an important health issue. Non-alcoholic steatohepatitis (NASH), which is a severe phenotype of NAFLD, is a disease that progresses to cirrhosis due to hepatocyte death and subsequent inflammation. The pathophysiology of NASH is related to lipotoxicity due to fat accumulation in the liver. Despite advances in the treatment of viral hepatitis, cirrhosis and liver-related deaths caused by NASH are thought to increase by 2030 and require urgent action [3,6]. Therefore, lipotoxicity in hepatocytes has been widely studied. Recently, it has been reported that cell death in NASH liver includes not only apoptosis but also non-apoptotic cell death such as necrosis and ferroptosis, but it is unclear which type of cell death is the most relevant to the pathophysiology of NASH [7–9].

Saturated fatty acids, such as palmitic acid, are highly cytotoxic, inducing apoptotic signals and impairing autophagy in hepatocytes [10–12]. In these processes, palmitic acid and toxic metabolites induce endoplasmic reticulum stress, JNK phosphorylation, and increased mitochondrial membrane permeability [13]. In contrast, unsaturated fatty acids, such as oleic acid, are thought to be less cytotoxic to hepatocytes. Furthermore, unsaturated fatty acids have been reported to reduce the toxicity of saturated fatty acids in hepatocytes [14].

Excessive consumption of high fructose corn syrup (HFCS) has led to an increase in the obese population [15–17]. The increased consumption of fructose-rich beverages is directly associated with the increase in the number of subjects with metabolic syndrome [15–17]. The metabolism of fructose differs to that of glucose in that most fructose metabolites flow into the downstream path-

* Corresponding author at: Keisuke Kakisaka, Division of Hepatology, Department of Internal Medicine, School of Medicine, Iwate Medical University, 1-1-1 Idaidori, Yahaba-cho, Iwate 0283694, Japan. Tel.: +81 19 651 5111; fax: +81 19 652 6664.
E-mail address: keikaki@iwate-med.ac.jp (K. Kakisaka).

https://doi.org/10.1016/j.jnutbio.2022.109052
0955-2863/© 2022 Elsevier Inc. All rights reserved.

way of glycolysis rather than to phosphofructokinase (PFK), the rate-limiting enzyme of the glycolytic system, and are not regulated by PFK. As a result, a higher fructose intake accelerates fatty acid synthesis, citric acid circuit turnover, and glycogenesis, leading to the development of dyslipidemia, atherosclerosis, and worsening of insulin resistance [18,19]. Fructose has also been reported to cause cytotoxicity through the production of reactive oxygen species (ROS) [20–22]. In a NASH rodent model, feeding sucrose, consisting of both glucose and fructose, to methionine-choline-deficient mice induces lobular inflammation in the liver [23]. Furthermore, a high-fat diet with sucrose decreased enzymes associated with phospholipids, and these changes enhanced lipotoxicity via caspase-independent hepatocyte death [24]. Fructose has been found to be more cytotoxic than glucose [23,25]. However, the toxicity of lipids and fructose in hepatocytes is not fully understood.

Accordingly, in this study, we aimed to elucidate the effects of fructose on lipotoxicity in cultured hepatocytes, mouse primary hepatocytes, and a NASH mouse and human model.

2. Materials and methods

2.1. Cells

Hepatoma cell-line: HepG2 cells were used as cultured hepatocytes. Primary mouse hepatocytes were isolated from male 10-week-old C57BL/6J mice (Charles River, Yokohama, Japan), using liver perfusion medium and liver digest medium (cat. no. 17701-038 and 17703-034; Gibco Life Technologies Corp, Carlsbad, CA, USA), according to the classic two-step protocol. Following anesthesia, the inferior vena cava was cannulated and the liver was perfused with liver perfusion medium (37°C). Following perfusion, the portal vein was cut and perfused with liver digest medium (pH 7.4, 37°C). The liver was removed and gently homogenized in Dulbecco's modified Eagle's medium (DMEM) with low glucose (cat. no. 11885084; Gibco). The liver cell suspension was homogenized with 20 mL of hepatocyte wash medium (cat. no. 17704-024; Gibco). The cell suspension was centrifuged at 50×*g* for 5 min, and the pellet was resuspended in 20 mL of medium. The cell suspension was filtered through a 100 μm cell strainer and centrifuged at 50×*g* for 5 min, before cell pellets were resuspended in Williams Medium E (cat. no. A12176; Gibco) containing 5% antibiotic–antimycotic mixed solution (cat. no. 02892-54; Nacalai Tesque, Kyoto, Japan). Cell viability, as determined by Trypan Blue exclusion, was generally >85%. After isolation, primary mouse hepatocytes were plated on collagen type I coated flat-bottom plates (cat. no. 11-0181-3; IWAKI Science Products Department, Shizuoka, Japan). Cells were maintained at 37°C in a humidified atmosphere of 5% CO_2.

These cell lines were maintained in low glucose DMEM (1 g/L) (cat. no. 11885084; Gibco) supplemented with 10% fetal bovine serum (cat. no. 26140-079; Gibco). Palmitic acid (PA; cat. no. P5585-10G; Sigma-Aldrich, St. Louis, MO, USA) and oleic acid (OA; cat no. O7501-5G; Sigma-Aldrich) were used with DMEM supplemented with either glucose (3.5 g/L; high glucose) or fructose (3.2 g/L; high fructose). These two media have equal energy per unit volume. PA and OA stock concentrations were 160 mM. The cells were treated with 400 or 800 μM of the indicated lipids to confirm lipid toxicity.

2.2. Cell proliferation assay

Cell proliferation was measured using Cell Count Reagent SF (cat. no. 07553-44; Nacalai Tesque), based on the 2-(2-methoxy-4-nitrophenyl)-3-(4-nitrophenyl)-5-(2,4-disulfophenyl)-2H-tetrazolium monosodium salt (WST-8) assay, and absorbance was determined using a microplate reader (Multiskan FC; Thermo Fisher Scientific, Waltham, MA, USA). Assays were performed according to the manufacturer's instructions. Briefly, cells were seeded into 96-well plates 24 h before observation. After removing the medium from each well, 100 μL medium with the indicated free fatty acids (FFAs), or solvent as a control, was added, and cells were incubated for 16 h. Cell Count Reagent SF (10 μL) was added to each well, and the absorbance at 450 nm was immediately measured as background absorbance. The cells carried out a color reaction in a CO_2 incubator for 2 h, and then the absorbance at 450 nm was measured. The background absorbance at 450 nm was subtracted. The ratio of absorbance relative to the control group was reported to determine cell proliferation.

2.3. Cell death assay

For the cell death assay, the Apoptotic/Necrotic Cell Detection Kit (cat. no. PK-CA707-30017, PromoCell GmbH, Heidelberg, Germany) was used to stain cells. Cells were seeded on glass coverslips of six-well flat-bottom plates and treated with different media. Following incubation for 15 min, the cells were visualized using a fluorescence microscope (EVOS Cell Imaging Systems, Thermo Fisher Scientific). The red staining represented necrotic cells and the green staining indicated apoptotic cells. Results were presented as the ratio of the number of stained sites to the number of nuclei (stained blue). The assay was performed at least three times.

2.4. Detection of ROS

Cells were seeded on glass coverslips of six-well flat-bottom plates and treated with different media. To assess ROS production in hepatocytes, CellROX Green Reagent (cat. no. 10422; Thermo Fisher Scientific) at a final concentration of 5 μM was added to each well. The cells were incubated at 37°C for 30 min. Following fixation in 3.7% formaldehyde for 15 min, cells on glass coverslips were then mounted with mounting medium containing 4,6-diamidino-2-phenylindole. The cells were visualized using a fluorescence microscope. The staining in green punctate dots were represented ROS. Results were presented as the ratio of the number of cells with punctate dots to the number of nuclei. The generation of ROS was measured in at least four high-power field images.

2.5. Immunoblotting analysis

Whole-cell lysates were prepared as previously described. Equal amounts of protein (20–40 μg) were resolved by sodium dodecyl sulfate-polyacrylamide gel electrophoresis on 4–12% acrylamide gels and transferred to nitrocellulose membranes (cat. no. 1620090; BIO-RAD Laboratories, Hercules, CA, USA). The membranes were incubated with primary antibodies at 4°C overnight and were then incubated with the appropriate horseradish peroxidase-conjugated secondary antibodies at 23±2°C for 60 min. Bound antibodies were visualized using an ImmunoStar LD (cat. no. 292-69903; FUJIFILM Wako Pure Chemical Corporation, Osaka, Japan). The bands were visualized and digitally captured on a C-Digit blot scanner (LI-COR, Lincoln, NE).

2.6. Animals

Male 4-week-old C57BL/6J mice were housed in humidity-controlled rooms with a 12-h light/12-h dark cycle at 22°C with *ad libitum* access to drinking water. After 1 week of habituation, three mice fed normal chow (Cont), four mice fed a high-fat diet (HFD; HFD-60; Oriental Yeast Co., Tokyo, Japan), and four mice fed an HFD with supplementation of sucrose (42 g/L; HFDS) were assigned and fed their respective diets for 16 weeks. All animal experiments were approved by the institutional board for Animal Care and Use Committee (Iwate Medical University: [Morioka, Japan; approval no. 28–001]). Serum alanine aminotransferase (ALT), aspartate aminotransferase (AST), and total cholesterol (TC) were measured with an autoanalyzer (cat. no. JCA-BM2250; JEOL, Tokyo, Japan).

2.7. Histological evaluation

Paraformaldehyde-fixed (4%), paraffin-embedded liver tissue blocks were cut into 3 μm-thick sections, and hematoxylin and eosin staining was used to evaluate steatosis, lobular inflammation, and hepatocyte ballooning, and to compare the NAFLD activity score (NAS) between the HFD and HFDS groups. Masson Goldner staining was used to observe fibrosis, hemoxygenase-1 (HO-1) staining for HO-1 expression, p-MLKL staining for MLKL phosphorylation, cleaved caspase-1 staining for Caspase-1 cleavage, TdT-mediated dUTP Nick End Labeling (TUNEL) assay for detecting of hepatocellular apoptosis.

2.8. Quantitative reverse transcription polymerase chain reaction (qRT-PCR)

Total cellular RNA was extracted using TRIzol reagent (cat. no. 12183555, Thermo Fisher Scientific) and was reverse transcribed into cDNA with Moloney murine leukemia virus reverse transcriptase (Invitrogen, Carlsbad, CA, USA) and random primers (Invitrogen). The cDNA was used as a template for qRT-PCR, which was carried out on a LightCycler instrument (Roche Applied Science) using Power SYBR Green PCR Master Mix (cat. no. 4367659, Thermo Fisher Scientific) as a fluorophore. Gene expression was quantified by the $2^{-\Delta\Delta Ct}$ method, and the target mRNA expression levels were expressed relative to glyceraldehyde 3-phosphate dehydrogenase in each sample. PCR primers are summarized in Table 1.

2.9. Liver histology and immunohistochemical analysis of human NAFLD patients

Liver specimens from eight NAFLD patients (NAFL; *n*=4, NASH; *n*=4) diagnosed by liver biopsy were used for immunohistochemical analysis. Patients were selected from among those who underwent liver biopsy due to clinical necessity at Iwate Medical University Hospital in Japan. NAFLD activity score (NAS) 1–4 was defined as NAFL (simple steatosis) and 5 or higher as NASH (Table 2). Patients with a history of excessive alcohol intake, other chronic liver diseases, and drug-induced fatty liver were excluded. The selection of patients and the experimental process were in compliance with the Declaration of Helsinki. The experimental protocol was approved

Table 1
PCR primers used in this study.

Gene	Forward or reverse primer	Primer sequence (5′–3′)
αSMA	Forward	ctctcttccagccatctttcat
αSMA	Reverse	tataggtggtttcgtggatgc
Collagen I	Forward	ccgctggtcaagatggtc
Collagen I	Reverse	ctccagcctttccaggttct
Collagen III	Forward	ctcctggtgagcgaggac
Collagen III	Reverse	gaccaggttgcccatcact
GAPDH	Forward	gggttcctataaatacggactgc
GAPDH	Reverse	ccattttgtctacgggacga

Table 2
Clinical scoring and immunohistochemical staining of liver biopsy specimens from human NAFL and NASH patients.

Sex	Age	Brunt (stage)	Brunt (grade)	NAS	Steatosis	Lobular inflammation	Hepatocyte ballooning	HO-1-positive cell counts/HPF	p-MLKL-positive cell counts/HPF
M	50	1	1	1	0	1	0	1	1
M	51	1	1	2	0	2	0	0	0
F	63	1	1	1	0	1	0	0	2
M	47	1	1	1	0	1	0	0	2
F	21	2	2	5	1	2	2	25	26
F	57	3	2	6	2	2	2	9	11
F	66	3	3	7	3	3	2	21	16
M	46	3	3	7	3	3	1	10	9

Abbreviations: HO-1, hemeoxygenase-1; HPF, high-power field; NAFL, non-alcoholic fatty liver; NAS, NAFLD activity score; NASH, non-alcoholic steatohepatitis; P-MLKL, phosphorylated mixed lineage kinase domain-like.

by the Ethics Review Committee of the Faculty of Medicine, Iwate Medical University (approval number: MH2020-171). Liver biopsy specimens were obtained from NAFL and NASH patients using a 16G needle biopsy kit according to the standard protocol. HO-1 staining for HO-1 expression and p-MLKL staining for MLKL phosphorylation was performed. The number of positive cells was measured in at least five high-power field images, and the median values were calculated.

2.10. Reagents and antibodies

For the cell proliferation assay, N-acetyl cysteine (NAC; cat. no. A9165-25G, Sigma-Aldrich) was used. NAC was dissolved in phosphate-buffered saline (pH 7.4, cat. no. 10010-023, Gibco) to obtain a 2 M stock solution.

The following primary antibodies were used for immunoblotting analysis and immunohistochemistry: goat anti-β-actin (1:1,000; cat. no. sc-1616; Santa Cruz Biotechnology, Santa Cruz, CA, USA), anti-cleaved caspase-3 (1:1,000; cat. no. 9661; Cell Signaling Technology), anti-cleaved caspase-1 (1:1,000; cat. no. 89332; Cell Signaling Technology), anti-p-MLKL for HepG2 cells (1:1,000; cat. no. 91689; Cell Signaling Technology), anti-p-MLKL for mouse primary hepatocytes (1:1,000; cat. no. ab196436; Abcam, Cambridge, UK), anti-HO-1 for immunohistochemistry (1:30 (mouse liver), 1:100 (human liver); cat. no. sc-136960; Santa Cruz Biotechnology), and anti-p-MLKL for human liver immunohistochemistry (1:400; cat. no. MAB9187-100; Bio-Techne, MN, USA), anti-cleaved caspase-1 for immunohistochemistry (1:30 (mouse liver; cat. no. PA5-38099; Thermo Fisher Scientific).

2.11. Statistical analysis

All data represent the results of at least three independent experiments. The data are expressed as mean±standard deviation values. Between-group comparisons were made using one-way analysis of variance with Student's *t* test and *post hoc* Dunnett's test. All statistical analyses were performed using the SPSS 17.0 software program (SPSS Inc., Chicago, IL, USA), and results were considered significant when the *P* value was $<.05$.

3. Results

3.1. Fructose-supplemented medium enhanced the cytotoxicity of OA

To evaluate how fructose affected lipotoxicity in hepatocytes *in vitro*, OA- and PA-toxicity were checked under the high glucose or high fructose environment using cell proliferation assays. PA-induced cytotoxicity in HepG2 cells was observed for both glucose-supplemented and fructose-supplemented media. In contrast, OA-induced cytotoxicity was only observed in cells cultured in fructose-supplemented medium (Fig. 1A).

3.2. OA-induced cytotoxicity in cells in fructose-supplemented medium was associated with necrotic cell death

To determine the pathophysiology by which fructose enhanced OA-induced cytotoxicity, the type of cell death in HepG2 cells was confirmed using fluorescence microscopy. PA induced apoptotic cell death in both glucose-supplemented and fructose-supplemented media, although the apoptotic cell death rate was higher in cells in glucose-supplemented medium (Fig. 1B). In contrast, necrotic cell death was significantly increased in HepG2 cells with OA treatment in fructose-supplemented medium (Fig. 1B).

3.3. NAC attenuated OA-induced necrotic cell death via prevention of OA-induced ROS production in cells cultured in fructose-supplemented medium

Based on previous studies that oxidative stress might be involved in the pathogenesis of NAFLD [26], we speculated that ROS might be involved in OA-induced cell death in the fructose-supplemented medium. ROS production was not increased in both glucose-supplemented and fructose-supplemented media without OA or PA (Fig. 1C). In contrast, OA increased ROS production in HepG2 cells cultured in fructose-supplemented medium. However, OA did not increase ROS production in HepG2 cell with glucose-supplemented medium. Although PA induced cell death, ROS production was not increased (Fig. 1C). Thus, we investigated the effects of NAC on OA-induced cytotoxicity in HepG2 cells cultured in the fructose-supplemented medium. NAC of 2 mM decreased ROS production in HepG2 cells cultured in OA-supplemented high-fructose medium (Fig. 1D). We also confirmed reproducibility in primary mouse hepatocytes, because HepG2 might have a

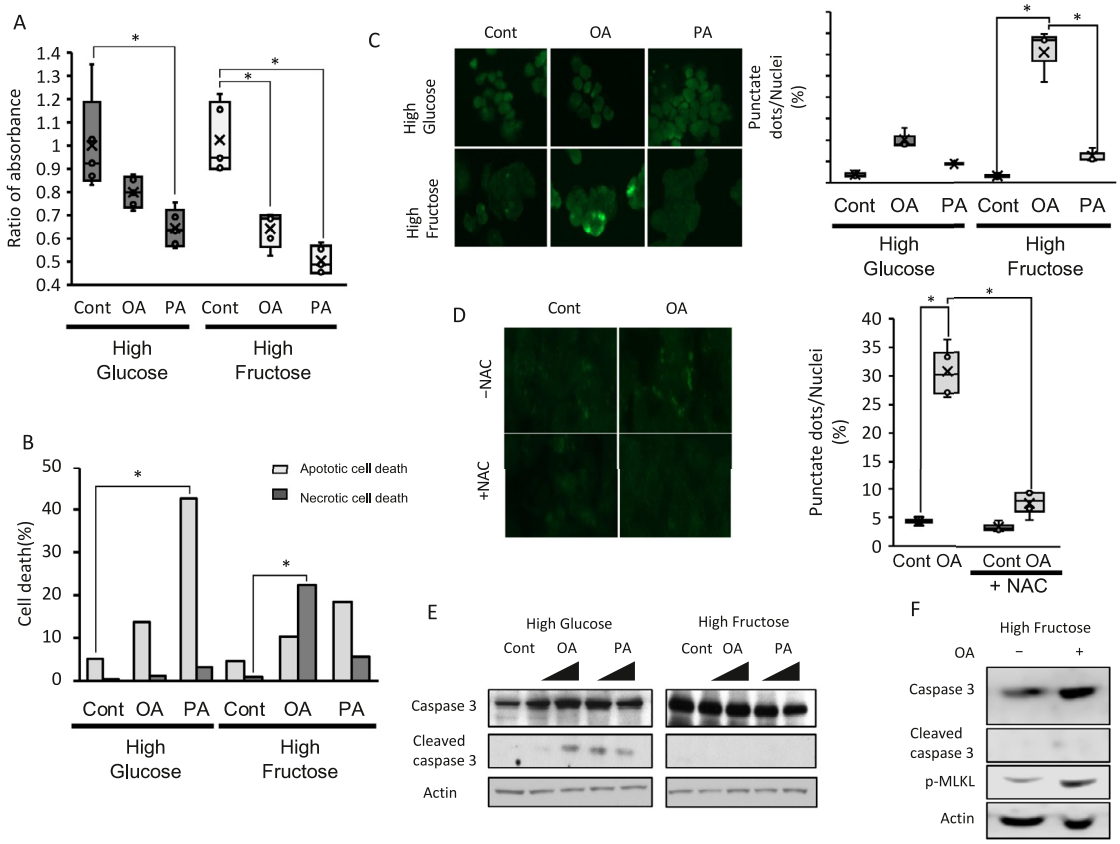

Fig. 1. Fructose intake increased OA-induced cytotoxicity via necroptosis and ROS production in HepG2 cells. N-acetylcysteine (NAC) decreased OA-induced ROS production. (A) HepG2 cells were incubated with OA or PA for 16 h. Vehicle-treated cells were used as control (Cont). Three conditions were evaluated in two different media: glucose-containing medium (high glucose) and fructose-containing medium (high fructose). We used SF reagent for the cell proliferation assay. (B) Apoptotic and necrotic cell death was detected by fluorescence microscopy using the Apoptotic/Necrotic/Healthy Cell Detection Kit. Results were presented as the ratio of the number of stained sites to the number of nuclei (stained blue). (C) ROS production was detected using CellROX Green Reagent, and images were obtained by fluorescence microscopy. Control (Cont), OA, and PA treated with glucose-containing medium (high glucose) or fructose-containing medium (high fructose). (D) Treatment of control (Cont) and OA in fructose-containing medium with or without NAC. Green staining in punctate dots represents ROS. Results were presented as the ratio of the number of cells with punctate dots to the number of nuclei. The generation of ROS was measured in at least four random high-power field images. Data represent the mean ± SD (*P<.05). (E) Immunoblot analysis of caspase-3, cleaved caspase-3, phosphorylated MLKL, and actin. Whole-cell lysates were prepared from HepG2 cells after incubation with OA, PA or control treatment for 8 h. (F) Whole-cell lysates were prepared from HepG2 cells after incubation with OA or control treatment for 8 h. Data represent the mean±SD (*P<.05).

metabolism specific to hepatoma cell lines. In mouse primary hepatocytes, OA with fructose-supplemented medium also increased necrotic cell death (Fig. 2A). In addition, the production of ROS was also enhanced under these conditions and NAC suppressed this cytotoxicity (Fig. 2B and C).

3.4. Fructose enhanced OA-induced cytotoxicity via a caspase-3-independent manner, induced cleavage of caspase-1 and necroptosis

To determine the mechanisms of enhanced cytotoxicity in cells with OA-supplementation in high-fructose supplemented, signaling pathways associated with lipotoxicity were evaluated in HepG2 cells and mouse primary hepatocytes using immunoblot analysis. In HepG2 cells, 800 μM OA and PA significantly induced the cleavage of caspase-3 in high glucose-supplemented medium. In contrast, cleaved caspase-3 did not increase in fructose-supplemented medium (Fig. 1E). In mouse primary hepatocytes, OA-induced cytotoxicity did not cleave caspase-3, but cleavage of caspase-1 occurred in the medium supplemented with fructose (Fig. 2D).

These data suggest that fructose enhanced OA cytotoxicity through a caspase-3-independent pathway and also induced cleavage of caspase-1, which is thought to be associated with inflammation in NASH. In both HepG2 cells and mouse primary hepatocytes, the phosphorylation of MLKL was enhanced under these conditions, indicating necroptosis, which is referred to as programmed necrosis (Figs. 1F and 2D).

3.5. HFD induced steatosis in mice, and sucrose supplementation enhanced HFD-induced liver inflammation and fibrosis

To confirm the effects of sucrose, mice fed with a HFDS were evaluated. We compared the results for changes in body weight, liver histology, and laboratory data among mice in control, the HFD, and HFDS groups. Body weight was significantly higher in mice in the HFD and HFDS groups than in mice in the Cont group (Fig. 3A). AST levels were higher in mice in the HFDS group than in mice in the Cont group, and ALT and TC levels were higher in mice in the HFD and HFDS groups than in mice in the Cont group (Fig. 3A). Histological evaluation revealed overt lipid accumulation in the livers of mice in both the HFD and HFDS groups (Fig. 3B). Furthermore, lymphocyte accumulation was abundantly found in the HFDS group. No advanced fibrosis was found in mice in the HFD and HFDS groups (Fig. 3B). However, mRNA expression of fibrosis markers: α-smooth muscle actin and collagen III, was higher in the livers of mice in the HFDS group than in the livers of mice in the Cont group, whereas collagen I expression did not differ among these mice (Fig. 3C). There was a significant differ-

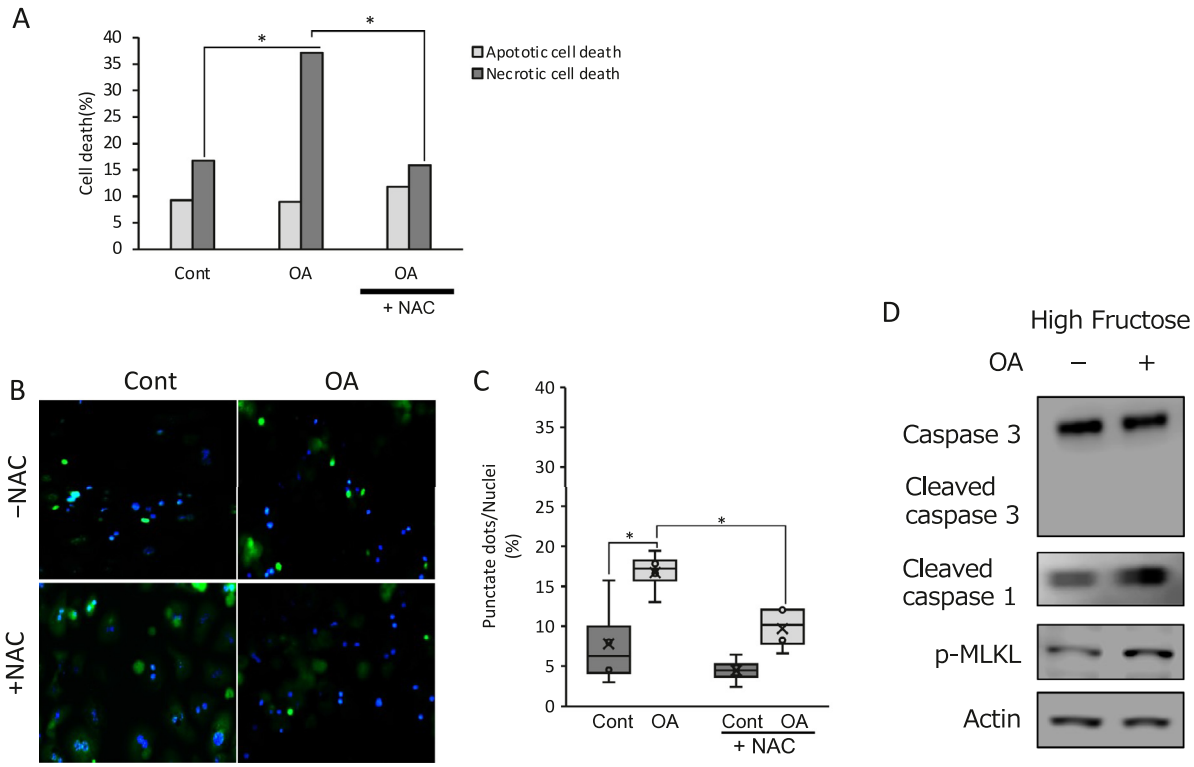

Fig. 2. Fructose-supplemented OA increased necroptosis, a planned caspase-independent necrosis, via phosphorylation of MLKL, and increased ROS production; NAC reduced OA-induced ROS production in primary mouse hepatocytes. (A) Apoptotic and necrotic cell death was detected by fluorescence microscopy using the Apoptotic/Necrotic/Healthy Cell Detection Kit. Results were presented as the ratio of the number of stained sites to the number of nuclei (stained blue). (B) ROS production was detected using CellROX Green Reagent, and images were obtained by fluorescence microscopy. Control (Cont) and OA treatment with fructose-containing medium with or without NAC. (C) Results were presented as the ratio of the number of cells with punctate dots to the number of nuclei. The generation of ROS was measured in at least four random high-power field images. Data represent the mean±SD (*P<.05). (D) Immunoblot analysis of caspase-3, cleaved caspase-3, cleaved caspase-1, phosphorylated MLKL, and β-actin. Whole-cell lysates were prepared from mouse primary hepatocytes after 8 h incubation with OA or control treatment.

ence in NAS scores for lobular inflammation and the total between the HFD and HFDS groups. The scores for ballooning and steatosis tended to be higher in the HFDS group, but the difference was not significant (Fig. 3D). These data indicated that HFDS in this study revealed steatohepatitis with fibrogenic changes, suggesting that this model may indicate a good model for early-stage NASH.

3.6. HFDS increased HO-1 expression, MLKL phosphorylation, cleavage of caspase-1 and the number of hepatocellular apoptosis in mouse liver

To elucidate whether supplementation of sucrose had similar effects of fructose on inducing ROS production and enhancing cytotoxicity due to necroptosis and cleavage of caspase-1 in an *in vivo* study also, we evaluated HO-1 expression, MLKL phosphorylation, cleavage of caspase-1, TUNEL assay in mouse liver. The positive area of HO-1, p-MLKL, cleaved caspase-1 staining in hepatocytes increased in mice in the HFDS group compared to mice in the Cont and HFD groups (Fig. 4A and B). Moreover, the number of TUNEL-positive cells was significantly increased in the HFDS group compared with the control and HFD groups.

3.7. HO-1 expression and MLKL phosphorylation were upregulated in human NASH liver

Based on *in vitro* and *in vivo* results, we evaluated the involvement of ROS and the presence of necroptosis in liver biopsy specimens from human NAFLD patients by immunohistochemical staining for HO-1 and p-MLKL (Fig. 5A). The number of HO-1- and p-MLKL-positive cells was markedly increased in NASH livers compared with NAFL livers (Table 2 and Fig. 5B). In particular, there were many ballooning hepatocytes around the central vein (zone 3) in the liver lobule, and these ballooning hepatocytes were positive for both HO-1 and p-MLKL. There was a positive correlation between the number of HO-1 positive cells and the number of p-MLKL positive cells, with a correlation coefficient of 0.522 (Fig. 5C).

4. Discussion

It has been reported that saturated fatty acids, such as PA, activate proapoptotic Bcl-2 proteins and induce JNK-dependent lipoapoptosis in hepatocytes [10], while unsaturated fatty acids, such as OA and PO, inhibit saturated fatty acid-induced cytotoxicity and ER stress. Thus, unsaturated fatty acids are considered to be less hepatocytotoxic than saturated fatty acids.

Surprisingly, in this study, OA enhanced hepatocytotoxicity through a caspase-3-independent necrotic cell death pathway and induced cleavage of caspase-1 in cells cultured in medium containing high concentrations of fructose. This cell death was inhibited by NAC, a scavenger of ROS, and mediated by MLKL phosphorylation, which is a key molecular trait of programmed cell death (necroptosis). In the subsequent *in vivo* study, sucrose supplementation induced liver inflammation, increased the expression of fibrosis markers, and led to a higher NAS score in mice fed a HFDS group. This result supports that sucrose, which contains fructose, induces liver injury, and promotes liver fibrosis. The expression of HO-1, a scavenger of ROS, was markedly increased in HFDS mice, which are considered to be a NASH mouse model. Similar to the

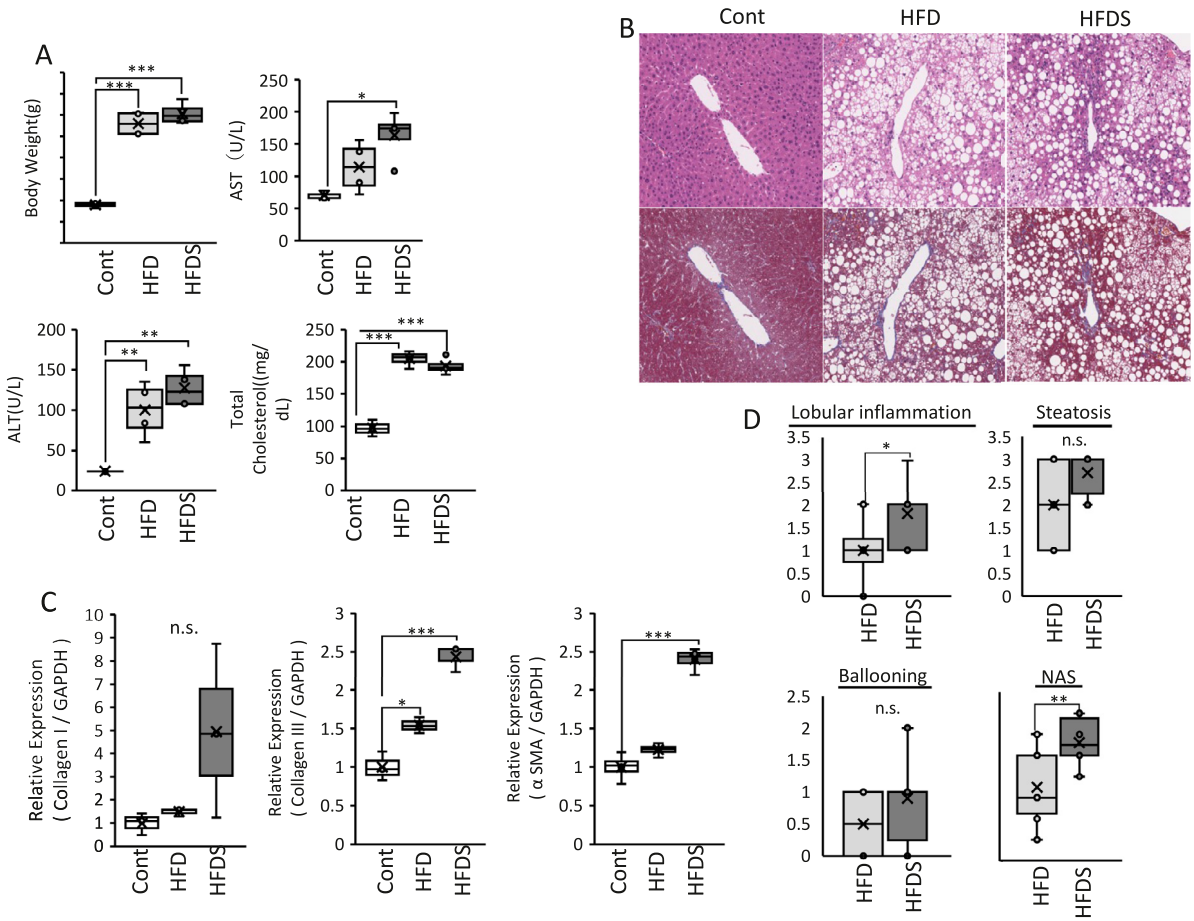

Fig. 3. Effects of HFD with or without sucrose on body weight, liver enzymes, hypercholesteremia, and liver histology. We evaluated the effects of HFD with or without sucrose on body weight, liver enzymes, hypercholesterolemia, and liver histology. (A) Body weight, aspartate aminotransferase, alanine aminotransferase, and total cholesterol were evaluated after 16 weeks of feeding mice with a normal (Cont), high-fat (HFD), or high-fat diet with sucrose (HFDS). (B) Representative micrographs of liver sections stained with hematoxylin and eosin and Masson's trichrome. Left, middle, and right are control, HFD, and HFDS groups, respectively. (C) mRNA expression of the indicated genes was analyzed by qRT-PCR. Data represent mean±SD (*P<.05). (D) Lobular inflammation, hepatocyte ballooning, and steatosis were evaluated, and NAFLD activity score (NAS) between HFD and HFDS groups were compared. Data represent mean±SD (*P<.05, **P<.01, ***P<.001).

results of the *in vitro* study, fructose supplementation induced hepatocyte damage via ROS production. Furthermore, phosphorylation of MLKL and cleavage of caspase-1 both increased in HFDS mice compared to that in HFDS mice. In addition, the number of TUNEL-positive cells was also increased in HFDS mice. As glucose in the HFD mice was sufficiently supplied in the diet, the significant findings regarding the HFDS mice were mainly due to fructose supplementation. Further investigation using human liver biopsy tissues showed that HO-1 expression and MLKL phosphorylation were upregulated in human NASH livers compared to human NAFL livers, especially within swollen hepatocytes. Based on these results, we concluded that high-fat, unsaturated fatty acids, and high fructose consumption induced the progression of NAFLD by inducing necroptosis via MLKL phosphorylation and ROS production.

Excess ROS causes lipid peroxidation of mitochondrial membranes, which contributes to impaired mitochondrial function and accelerates the production of additional ROS. Oxidative stress also triggers the production of inflammatory cytokines, leading to inflammation, and fibrogenesis, which contribute to the development of NASH [27]. In the livers of Nrf2-null mice fed a methionine- and choline-deficient diet, glutathione and catalase decreased and ROS levels increased; these mice rapidly developed steatohepatitis [28]. Conversely, it has been reported that the addition of dietary NAC to a NASH rat model attenuated the decrease in hepatic GSH levels and suppressed hepatocellular damage and liver fibrosis [29]. Additionally, NAC was found to alleviate oxidative stress by decreasing lipid peroxidation and increasing GSH in several NASH mouse models. These models also showed a decrease in pro-inflammatory cytokines and in the number of apoptotic cells [30]. Taken together, NAC supplementation reduces cytotoxicity and limits NASH progression.

It has been reported that activation of caspase-1 and interleukin-1β in the MCD-fed mouse model of NASH causes marked steatohepatitis and fibrosis, and that expression of genes involved in inflammation, fibrosis, and lipogenesis is significantly reduced in caspase-1 knockout mice [31,32]. In addition, it has been shown that activation of caspase-1 mobilizes neutrophils to the liver and that myeloperoxidase enhances oxidative stress and fibrosis [33,34]. In the present study, fructose did not activate caspase-3, but enhanced the hepatocytotoxicity of OA, probably due to induction of inflammatory cells and enhancement of oxidative stress through activation of caspase-1.

Necroptosis is a programmed cell death that occurs in response to various stimulations, such as TNF-α, resulting in the ballooning of intracellular organelles and disruption of cell membranes. Necroptosis is generally initiated by reciprocal phosphorylation between receptor-interacting protein 1 (RIP1) and 3 (RIP3), which is required for necrosome assembly and activation of necroptosis signaling. Phosphorylated RIP3 recruits and phosphorylates MLKL, which is the most downstream protein in the necroptosis signaling

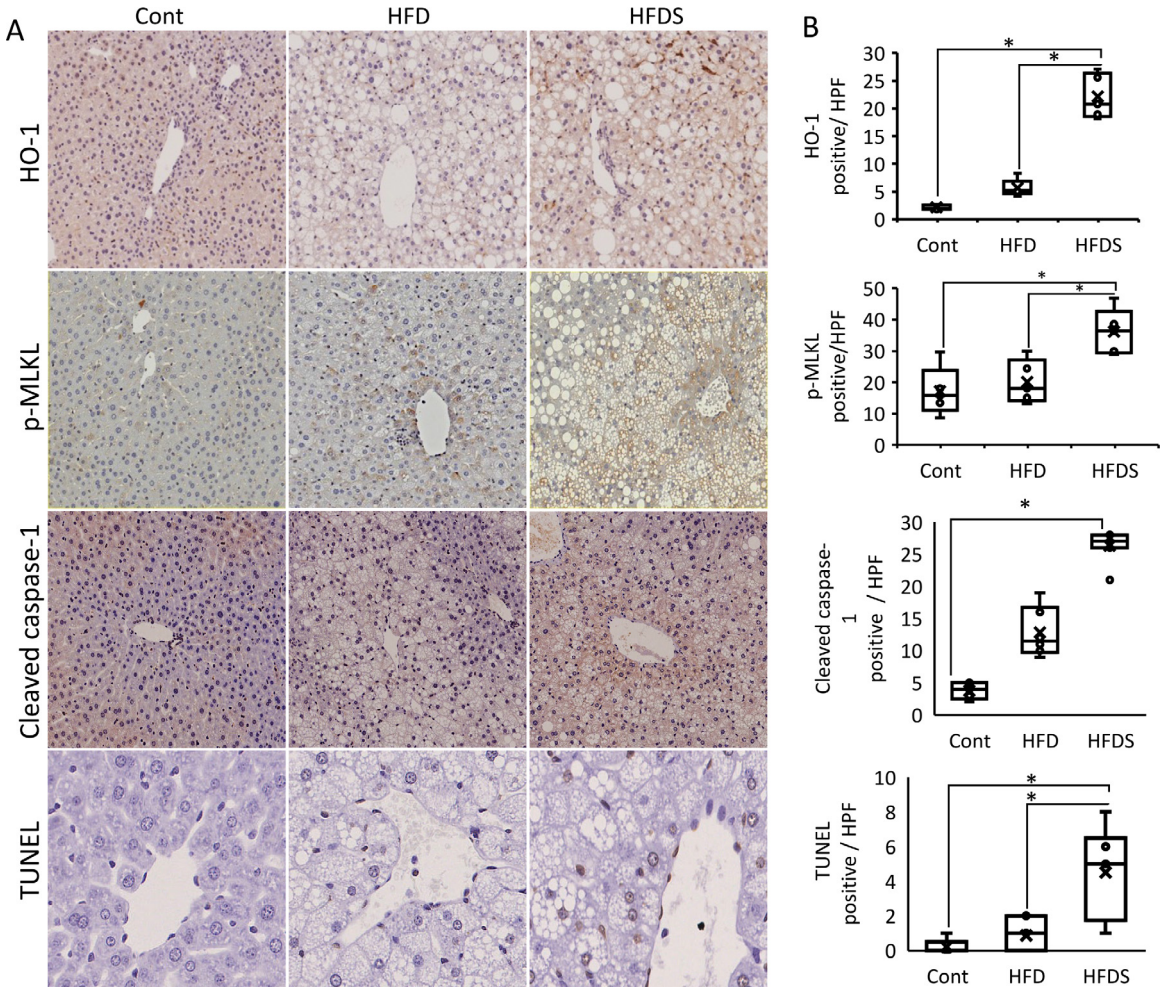

Fig. 4. HO-1 and p-MLKL levels in the liver were elevated in HFDS-fed mice. (A) Immunohistochemical analysis of HO-1, p-MLKL, cleaved caspase-1, and TUNEL assay. The left, middle, and right panels represent groups fed normal (Cont), a high-fat (HFD), or a high-fat diet with sucrose (HFDS), respectively. (B) Stain-positive hepatocytes (HO-1 (top row), p-MLKL (second row from top), cleaved caspase-1 (second row from bottom), TUNEL (bottom row)) were counted in at least five random high-power field images. Data represent mean±SD (*P<.05).

pathway. It has been reported that mitochondrial ROS promotes necroptosis, and activated RIP3 induces additional phosphorylation of MLKL and ROS production, forming a positive necroptosis feedback loop [35,36].

In NASH model mice fed a high-fat/high energy diet and high-fructose water, necroptosis occurred rapidly, leading to inflammatory reactions and fibrosis in the liver [37,38]. These data support the findings of the present study, which that show that a high-fructose environment causes necroptosis in hepatocytes via oxidative stress, leading to NASH. Thus, it is important to control oxidative stress to suppress the progression of necroptosis and subsequent development of NASH.

Lipid metabolism in the liver is complex, and although PA is known to be a strong inducer of apoptosis *in vitro*, NASH model mice fed PA did not show a similar response [39]. In contrast, HFD mice that were injected with an emulsion of PA developed liver inflammation. These results suggest that dietary PA did not induce liver toxicity, as PA was metabolized in the liver after absorption from the small intestine [40]. Thus, identification of toxic fatty acids in the liver is challenging. Lipidomics in a liver sample showed that several fatty acid components were increased in NASH liver tissues [41], and OA was identified as one of these fatty acids. These results support the results of the present study.

Hepatocyte ballooning is among the NAS components used to assess the severity of NAFLD. Hepatocyte ballooning has been reported to be a risk factor for fibrosis progression and play an important role in the pathogenesis of NASH [42,43]. However, the detailed mechanism underlying hepatocyte ballooning remains unclear. It is known that hepatocytes ballooning due to the accumulation of lipids, oxidized phospholipids, and ubiquitinated proteins in the cells, and that they lose their polarity due to the loss of keratin 8/18. Moreover, swollen hepatocytes secrete sonic hedgehog to escape cellular processing by autophagy, and the expression of caspase-9 is reduced, which prevents activation of the apoptotic pathway [44]. Taken together, swollen hepatocytes are considered to be undead cells, having escaped from cell death. In this study, we found that HO-1 expression and MLKL phosphorylation were increased in swollen hepatocytes in human NASH liver tissues. Increased ROS production was associated with this ballooning, suggesting that necroptosis may be one of the cell deaths that ultimately occur in swollen hepatocytes.

There were several limitations to this study. First, this study could not prove the up-regulation of phosphorylated RIP3, which phosphorylates MLKL. However, it has been reported that MLKL is the most downstream protein in the necroptosis pathway. Here, p-MLKL was used to show increased OA lipotoxicity and induction

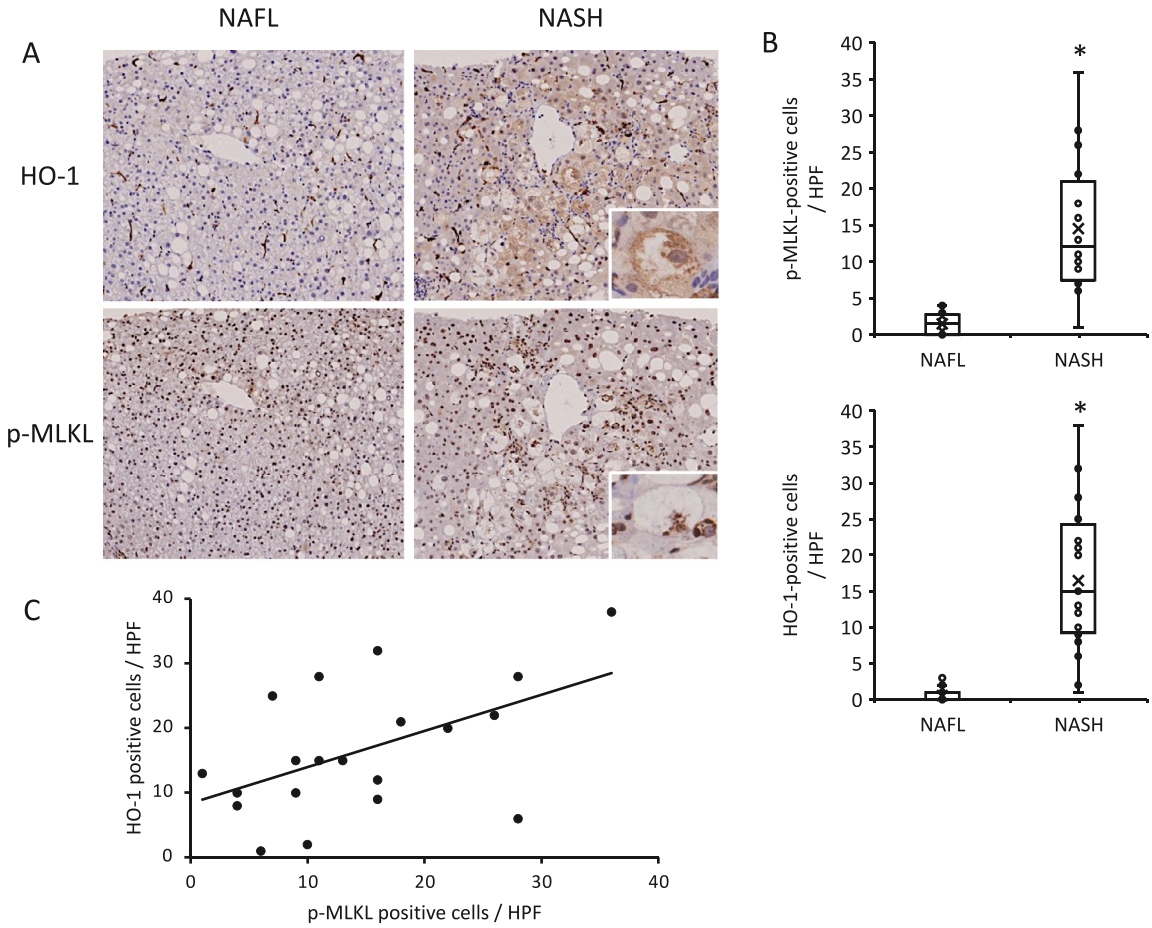

Fig. 5. HO-1 expression and MLKL phosphorylation were upregulated in human NASH liver tissues. (A) Immunohistochemical analysis of HO-1 and p-MLKL. Left, right panels indicate NAFL groups (NAFL) and NASH groups (NASH), respectively. (B) Immunohistochemical analysis of HO-1- and p-MLKL-positive hepatocyte counts. HO-1- and p-MLKL-positive hepatocytes were counted in at least five random high-power field images. Data are presented as the mean±SD (*P<.05). (C) Correlation between the number of HO-1- and p-MLKL-positive cells.

of necroptosis by fructose. Second, we showed that HO-1 expression was increased in response to increased ROS production, but we did not perform over-induction or silencing of HO-1 due to lack of samples. Since the administration of N-acetylcysteine scavenges ROS and suppresses cell death in cell experiments, further studies are needed on the enhanced expression of the ROS scavenging system and to determine how the combination of excess fructose and OA increases the generation of ROS.

Overall, the findings of this study showed that fructose enhanced OA lipotoxicity through the production of ROS and caused necroptosis in hepatocytes. NAC treatment and regulation of the necroptosis signaling pathway are potential targets for future NASH therapy.

Author contributions

I, Keisuke Kakisaka, the corresponding author of the work certify that all authors have participated sufficiently in the conception and design of the work and were involved in the acquisition of data. All of them have also participated in the analysis and interpretation of the data, as well as drafting the work. All authors also revised the work and contributed to the final approval of the version for publication. Each author also agreed to be accountable for all aspects of the work in ensuring that questions related to the accuracy or integrity of any part of the work are appropriately investigated and resolved.

While each author was involved in all the aspects above, specific authors carried a greater burden of responsibility as follows:

As principal investigator, Jo Kanazawa had full access to all the data in the study and takes responsibility for the integrity of the data and the accuracy of the data analysis.

Keisuke Kakisaka and Jo Kanazawa developed the study concept and design of the work.

Keisuke Kakisaka obtained funding.

Keisuke Kakisaka and Jo Kanazawa recruited patients and acquired data.

Jo Kanazawa produced the figures.

Jo Kanazawa statistically interpreted the data.

Jo Kanazawa drafted the work.

Yuji Suzuki, Takehiro Yonezawa, Hiroaki Abe, Ting Wang, and Yasuhiro Takikawa revised the work critically for important intellectual content.

Declaration of competing interests

The authors declare that there are no conflicts of interest.

Funding

This study was supported in part by a Grant-in-Aid for Scientific Research ©, awarded to K.K. [Grant no. 18K07980].

Supplementary materials

Supplementary material associated with this article can be found, in the online version, at doi:10.1016/j.jnutbio.2022.109052.

References

[1] Chooi YC, Ding C, Magkos F. The epidemiology of obesity. Metabolism 2019;92:6–10. doi:10.1016/j.metabol.2018.09.005.

[2] Shin D, Kongpakpaisarn K, Bohra C. Trends in the prevalence of metabolic syndrome and its components in the United States 2007–2014. Int J Cardiol 2018;259:216–19. doi:10.1016/j.ijcard.2018.01.139.

[3] Estes C, Razavi H, Loomba R, Younossi Z, Sanyal AJ. Modeling the epidemic of nonalcoholic fatty liver disease demonstrates an exponential increase in burden of disease. Hepatology 2018;67:123–33. doi:10.1002/hep.29466.

[4] Kanwal F, Kramer JR, Duan Z, Yu X, White D, El-Serag HB. Trends in the burden of nonalcoholic fatty liver disease in a United States Cohort of Veterans. Clin Gastroenterol Hepatol 2016;14:301–8 e2. doi:10.1016/j.cgh.2015.08.010.

[5] Chen Q, Ayer T, Bethea E, Kanwal F, Wang X, Roberts M, et al. Changes in hepatitis C burden and treatment trends in Europe during the era of direct-acting antivirals: a modelling study. BMJ Open 2019;9:1–11. doi:10.1136/bmjopen-2018-026726.

[6] Estes C, Anstee QM, Arias-Loste MT, Bantel H, Bellentani S, Caballeria J, et al. Modeling NAFLD disease burden in China, France, Germany, Italy, Japan, Spain, United Kingdom, and United States for the period 2016–2030. J Hepatol 2018;69:896–904. doi:10.1016/j.jhep.2018.05.036.

[7] Tsurusaki S, Tsuchiya Y, Koumura T, Nakasone M, Sakamoto T, Matsuoka M, et al. Hepatic ferroptosis plays an important role as the trigger for initiating inflammation in nonalcoholic steatohepatitis. Cell Death Dis 2019;10. doi:10.1038/s41419-019-1678-y.

[8] Xie Y, Hou W, Song X, Yu Y, Huang J, Sun X, et al. Ferroptosis: process and function. Cell Death Differ 2016;23:369–79. doi:10.1038/cdd.2015.158.

[9] Akazawa Y, Nakao K. To die or not to die: death signaling in nonalcoholic fatty liver disease. J Gastroenterol 2018;53:893–906. doi:10.1007/s00535-018-1451-5.

[10] Malhi H, Bronk SF, Werneburg NW, Gores GJ. Free fatty acids induce JNK-dependent hepatocyte lipoapoptosis. J Biol Chem 2006;281:12093–101. doi:10.1074/jbc.M510660200.

[11] Suzuki A, Kakisaka K, Suzuki Y, Wang T, Takikawa Y. C-Jun N-terminal kinase-mediated Rubicon expression enhances hepatocyte lipoapoptosis and promotes hepatocyte ballooning. World J Gastroenterol 2016;22:6509–16. doi:10.3748/wjg.v22.i28.6509.

[12] Tanaka S, Hikita H, Tatsumi T, Sakamori R, Nozaki Y, Sakane S, et al. Rubicon inhibits autophagy and accelerates hepatocyte apoptosis and lipid accumulation in nonalcoholic fatty liver disease in mice. Hepatology 2016;64:1994–2014. doi:10.1002/hep.28820.

[13] Kakisaka K, Cazanave SC, Fingas CD, Guicciardi ME, Bronk SF, Werneburg NW, et al. Mechanisms of lysophosphatidylcholine-induced hepatocyte lipoapoptosis. Am J Physiol - Gastrointest Liver Physiol 2012;302:77–84. doi:10.1152/ajpgi.00301.2011.

[14] Akazawa Y, Cazanave S, Mott JL, Elmi N, Bronk SF, Kohno S, et al. Palmitoleate attenuates palmitate-induced Bim and PUMA up-regulation and hepatocyte lipoapoptosis. J Hepatol 2010;52:586–93. doi:10.1016/j.jhep.2010.01.003.

[15] Basciano H, Federico L, Adeli K. Fructose, insulin resistance, and metabolic dyslipidemia. Nutr Metab 2005;2:1–14. doi:10.1186/1743-7075-2-5.

[16] Dhingra R, Sullivan L, Jacques PF, Wang TJ, Fox CS, Meigs JB, et al. Soft drink consumption and risk of developing cardiometabolic risk factors and the metabolic syndrome in middle-aged adults in the community. Circulation 2007;116:480–8. doi:10.1161/CIRCULATIONAHA.107.689935.

[17] Basaranoglu M, Basaranoglu G, Bugianesi E. Carbohydrate intake and nonalcoholic fatty liver disease: fructose as a weapon of mass destruction. Hepatobiliary Surg Nutr 2015;4:109–16. doi:10.3978/j.issn.2304-3881.2014.11.05.

[18] Hannou SA, Mckeown NM, Herman MA, Hannou SA, Haslam DE, Mckeown NM, et al. Fructose metabolism and metabolic disease. Find the latest version. Fructose Metab Metabol Dis 2018;128:545–55.

[19] Aeberli I, Hochuli M, Gerber PA, Sze L, Murer SB, Tappy L, et al. Moderate amounts of fructose consumption impair insulin sensitivity in healthy young men: a randomized controlled trial. Diabetes Care 2013;36:150–6. doi:10.2337/dc12-0540.

[20] Madlala HP, Maarman GJ, Ojuka E. Uric acid and transforming growth factor in fructose-induced production of reactive oxygen species in skeletal muscle. Nutr Rev 2016;74:259–66. doi:10.1093/nutrit/nuv111.

[21] Lim JS, Mietus-Snyder M, Valente A, Schwarz JM, Lustig RH. The role of fructose in the pathogenesis of NAFLD and the metabolic syndrome. Nat Rev Gastroenterol Hepatol 2010;7:251–64. doi:10.1038/nrgastro.2010.41.

[22] Léveillé M, Estall JL. Mitochondrial dysfunction in the transition from NASH to HCC. Metabolites 2019;9. doi:10.3390/metabo9100233.

[23] Pickens MK, Yan JS, Ng RK, Ogata H, Grenert JP, Beysen C, et al. Dietary sucrose is essential to the development of liver injury in the methionine-choline-deficient model of steatohepatitis. J Lipid Res 2009;50:2072–82. doi:10.1194/jlr.M900022-JLR200.

[24] Kakisaka K, Suzuki Y, Fujiwara Y, Suzuki A, Kanazawa J, Takikawa Y. Caspase-independent hepatocyte death: a result of the decrease of lysophosphatidylcholine acyltransferase 3 in non-alcoholic steatohepatitis. J Gastroenterol Hepatol 2019;34:1256–62. doi:10.1111/jgh.14461.

[25] Pickens MK, Ogata H, Soon RK, Grenert JP, Maher JJ. Dietary fructose exacerbates hepatocellular injury when incorporated into a methionine-choline-deficient diet. Liver Int 2010;30:1229–39. doi:10.1111/j.1478-3231.2010.02285.x.

[26] Raffaele M, Carota G, Sferrazzo G, Licari M, Barbagallo I, Sorrenti V, et al. Inhibition of heme oxygenase antioxidant activity exacerbates hepatic steatosis and fibrosis in vitro. Antioxidants 2019;8:277. doi:10.3390/antiox8080277.

[27] Nassir F, Ibdah JA. Role of mitochondria in nonalcoholic fatty liver disease. Int J Mol Sci 2015;15:8713–42. doi:10.3390/ijms15058713.

[28] Sugimoto H, Okada K, Shoda J, Warabi E, Ishige K, Ueda T, et al. Deletion of nuclear factor-E2-related factor-2 leads to rapid onset and progression of nutritional steatohepatitis in mice. Am J Physiol - Gastrointest Liver Physiol 2010;298:283–94. doi:10.1152/ajpgi.00296.2009.

[29] Kuang GG-MS-Q, O'Brien S, Thomas D, Hagop Kantarjian HY. N-acetylcysteine attenuates progression of liver pathology in a rat model of non-alcoholic steatohepatitis. J Nutr 2008;138:1872–9.

[30] Cayuela NC, Koike MK, Jacysyn J de F, Rasslan R, Cerqueira ARA, Costa SKP, et al. N-acetylcysteine reduced ischemia and reperfusion damage associated with steatohepatitis in mice. Int J Mol Sci 2020;21:1–19. doi:10.3390/ijms21114106.

[31] Dixon LJ, Flask CA, Papouchado BG, Feldstein AE, Nagy LE. Caspase-1 as a central regulator of high fat diet-induced non-alcoholic steatohepatitis. PLoS One 2013;8:1–10. doi:10.1371/journal.pone.0056100.

[32] Dixon LJ, Berk M, Thapaliya S, Papouchado BG, Feldstein AE. Caspase-1-mediated regulation of fibrogenesis in diet-induced steatohepatitis. Lab Investig 2012;92:713–23. doi:10.1038/labinvest.2012.45.

[33] Pulli B, Ali M, Iwamoto Y, Zeller MWG, Schob S, Linnoila JJ, et al. Myeloperoxidase-hepatocyte-stellate cell cross talk promotes hepatocyte injury and fibrosis in experimental nonalcoholic steatohepatitis. Antioxidants Redox Signal 2015;23:1255–69. doi:10.1089/ars.2014.6108.

[34] Xu R, Huang H, Zhang Z, Wang FS. The role of neutrophils in the development of liver diseases. Cell Mol Immunol 2014;11:224–31. doi:10.1038/cmi.2014.2.

[35] Zhang Y, Su SS, Zhao S, Yang Z, Zhong CQ, Chen X, et al. RIP1 autophosphorylation is promoted by mitochondrial ROS and is essential for RIP3 recruitment into necrosome. Nat Commun 2017;8:1–14. doi:10.1038/ncomms14329.

[36] Afonso MB, Rodrigues PM, Carvalho T, Caridade M, Borralho P, Cortez-Pinto H, et al. Necroptosis is a key pathogenic event in human and experimental murine models of non-alcoholic steatohepatitis. Clin Sci 2015;129:721–39. doi:10.1042/CS20140732.

[37] Liu XJ, Duan NN, Liu C, Niu C, Liu XP, Wu J. Characterization of a murine non-alcoholic steatohepatitis model induced by high fat high calorie diet plus fructose and glucose in drinking water. Lab Investig 2018;98:1184–99. doi:10.1038/s41374-018-0074-z.

[38] Wu X, Poulsen KL, Sanz-Garcia C, Huang E, McMullen MR, Roychowdhury S, et al. MLKL-dependent signaling regulates autophagic flux in a murine model of non-alcohol-associated fatty liver and steatohepatitis. J Hepatol 2020;73:616–27. doi:10.1016/j.jhep.2020.03.023.

[39] Farrell G, Schattenberg JM, Leclercq I, Yeh MM, Goldin R, Teoh N, et al. Mouse models of nonalcoholic steatohepatitis: toward optimization of their relevance to human nonalcoholic steatohepatitis. Hepatology 2019;69:2241–57. doi:10.1002/hep.30333.

[40] Ogawa Y, Imajo K, Honda Y, Kessoku T, Tomeno W, Kato S, et al. Palmitate-induced lipotoxicity is crucial for the pathogenesis of nonalcoholic fatty liver disease in cooperation with gut-derived endotoxin. Sci Rep 2018;8:1–14. doi:10.1038/s41598-018-29735-6.

[41] Allard JP, Aghdassi E, Mohammed S, Raman M, Avand G, Arendt BM, et al. Nutritional assessment and hepatic fatty acid composition in non-alcoholic fatty liver disease (NAFLD): a cross-sectional study. J Hepatol 2008;48:300–7. doi:10.1016/j.jhep.2007.09.009.

[42] Kakisaka K, Suzuki Y, Fujiwara Y, Abe T. Evaluation of ballooned hepatocytes as a risk factor for future progression of fibrosis in patients with non-alcoholic fatty liver disease. J Gastroenterol 2018;53:1285–91. doi:10.1007/s00535-018-1468-9.

[43] MacHado MV, Diehl AM. Pathogenesis of nonalcoholic steatohepatitis. Gastroenterology 2016;150:1769–77. doi:10.1053/j.gastro.2016.02.066.

[44] Hirsova P, Gores GJ. Ballooned hepatocytes, undead cells, sonic hedgehog, and vitamin E: therapeutic implications for nonalcoholic steatohepatitis. Hepatology 2015;61:15–17. doi:10.1002/hep.27279.